IEEE Robotics and Automation Letters (RAL) paper presented at the
2020 IEEE/RSJ International Conference on Intelligent Robots and Systems (IROS)
October 25-29, 2020, Las Vegas, NV, USA (Virtual)

Subject-Independent sEMG Pattern Recognition by Using a Muscle Source Activation Model

Minjae Kim[1], *Member, IEEE,* Wan Kyun Chung[2], *Fellow, IEEE,* and Keehoon Kim[2], *Member, IEEE*

***Abstract*— The interpretation of surface electromyographic (sEMG) signals facilitates intuitive gesture recognition. However, sEMG signals are highly dependent on measurement conditions. The relationship between sEMG signals and gestures identified from a specific subject cannot be applied to other subjects owing to anatomical differences between the subjects. Furthermore, an sEMG signal varies even according to the electrode placement on the same subject. These limitations reduce the practicability of sEMG signal applications. This paper proposes a subject-independent gesture recognition method based on a muscle source activation model; a reference source model facilitates parameter transfer from a specific subject, i.e., *donor* to any subject, *donee*. The proposed method can compensate for the angular difference of the interface between subjects. A *donee* only needs to perform ulnar deviation for approximately $2\,\mathrm{s}$ for the overall process. Ten subjects participated in the experiment, and the results show that, in the best configuration, the subject-independent classifier achieved a reasonable accuracy of $78.3\,\%$ compared with the subject-specific classifier $(88.7\,\%)$ for four wrist/hand motions.**

I. Introduction

Surface electromyographic (sEMG) signals contain information on muscular contractions that can be used to predict motion intention. As such, various robotics applications [1]–[3] have adopted sEMG signal-based pattern recognition.

However, the complex characteristics of sEMG signals have limited their applications. An sEMG signal recorded during a muscle contraction is highly dependent on the electrode placement. Thus, the placement of electrodes should be carefully done to obtain reliable signals representing the target motion; even a small displacement can cause significant performance degradation [4]. For these reasons, prostheses, one of the major applications of sEMG interfaces, have adopted a socket interface [5] that is tailored to users' specific needs based on their anatomical factors.

Most of all, a trained model for a specific user cannot be applied to another user owing to anatomical differences between the subjects, e.g., muscle parameters, including muscle thickness [6] and innervation zone location [7], [8].

This work was supported in part by the National Research Foundation of Korea (NRF) through the Global Frontier R&D Program on <Human-centered Interaction for Coexistence> funded by the Korean Government (Ministry of Science and ICT) under Grant NRF-M1AXA003-2010-0029748, and in part by the NRF through the convergence technology development program for bionic arm funded by the Ministry of Science and ICT under Grant 2014M3C1B2048419.

[1]Minjae Kim is with the Interaction and Robotics Research Center, Korea Institute of Science and Technology (KIST), South Korea `minjaekim@kist.re.kr`

[2]Wan Kyun Chung and Keehoon Kim are with the Department of Mechanical Engineering, Pohang University of Science and Technology (POSTECH), South Korea `wkchung@postech.ac.kr`; `khk@postech.ac.kr`

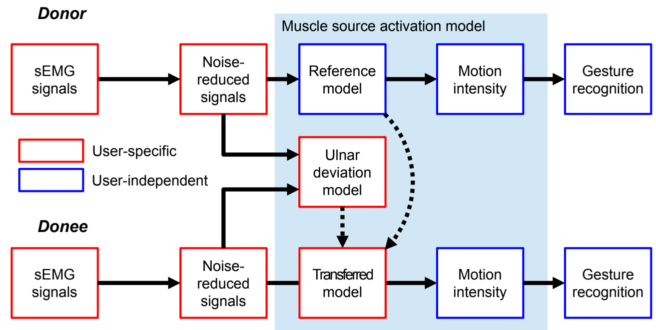

Fig. 1. Overall diagram of the subject-independent gesture recognition method based on a muscle source activation model.

Several techniques [9], [10], such as deep learning-based transfer learning [11], have been proposed to address the aforementioned problems. However, these model adaptations require the subject to perform all the target motions, which is time-consuming.

In this paper, we propose an automatic signal compensation method. A trained pattern recognition model for a specific user can be applied to other users by compensating for the sEMG signals. The proposed method includes our previous works: a muscle source activation model [12]–[15], a motion intensity extraction method [15], and a noise reduction method [15].

Fig. 1 presents overall diagram of the proposed method. First, baseline noise is removed to minimize environmental factors, such as skin conditions. Then, a muscle source activation model, motion intensity model, and motion intensity-based classifier are computed. In addition to this, the parameter transfer of the muscle source activation model is applied, which is a new method that facilitates the application of these models to other subjects.

The principle of parameter transfer involves the use of a reference model. In our previous muscle source activation model, all the source parameters were automatically calculated according to the anatomical factors of a subject; hence, a trained model on a subject cannot be applied to other subjects owing to anatomical differences between subjects; as a result, significantly poor performance was observed. To resolve this issue, additional constraints are added. The number of sources were set to four, and the sources were evenly distributed. The muscle source activation model consisting of these predefined source parameters will be referred to as the reference model. Although the use of a reference model may reduce the signal decomposition performance compared with that of a user-specific model, the reference mode has sufficient versatility to apply to other users. Thus, the parameter transfer requires only a simple motion of approximately $2\,\mathrm{s}$, as applied to subject-specific rotation compensation [13].

To demonstrate the proposed method, four hand motions were considered: wrist flexion (w/e), wrist extension (w/e), hand close (h/c), and hand open (h/o). Both a muscle source activation model with a motion intensity model and a pattern recognition model were trained on three subjects, and then fitted to other subjects (all 10 subjects) by performing ulnar deviation (u/d).

The proposed method has several advantages in teleoperation and prosthesis control applications.

In the case of teleoperation, the proposed method facilitates plug-and-play motion recognition for complex tasks beyond the simple command [16], [17] control. In addition, a user is not required to pay attention to align the interface rotation; the proposed method can compensate for the full-range of rotation [13], whereas conventional methods can only compensate for small displacements [18].

In the case of prosthesis control, a larger bank of *donors* may prevent the need to identify recognition model parameters from scratch. During the calibration procedure, a small subset of motions will be sufficient for the calibration of all motions at once; and the calibration takes only a few seconds. These benefits will enhance the efficiency of sEMG-based pattern recognition algorithms [19], such as prosthesis-guided-training [20]; these conventional methods require users to perform muscle contractions corresponding to the motions that need to be calibrated.

II. Methods

A. Subjects

A total of 10 subjects participated in the experiments. The subjects were divided into two groups. Those in group A (subjects 1–3) were familiar with sEMG signal processing, i.e., they had experience measuring sEMG signals for research purposes. Subjects 1, 2, and 3 were proficient in that order. On the other hand, the subjects in group B (subjects 4–10) did not have measuring experience. Subjects in groups A and B will be referred to as the *donors* and *donees*, respectively.

Reference models were constructed using sEMG signals from *donors*, and the signals measured from *donees* were used for performance evaluation. One of the purposes of the study is to demonstrate the applicability of the proposed method to users who are not familiar with sEMG signal measurement. Therefore, the guidance given to *donees* was minimized.

The experiments were approved by the Institutional Review Board of the Korea Institute of Science and Technology, Seoul, Korea.

B. Experimental Setup

sEMG signals were measured using an MYO armband (Thalmic Labs Inc., Kitchener, Canada), which consists of eight bipolar sEMG channels that can be wrapped around the forearm. An integrated inertial measurement unit (IMU) was used to compute the forearm orientation. If subjects maintained the same postures during the model initialization process, then the angular differences between subjects can be calculated. The differences can also be used as the initial value for the rotation compensation.

The sampling frequencies of the sEMG and IMU signals are $200\,\mathrm{Hz}$ and $50\,\mathrm{Hz}$, respectively, according to the limited bandwidth of the MYO armband. Measured signals were divided into windows of $200\,\mathrm{ms}$ and extracted every $25\,\mathrm{ms}$; the selected window length was acceptable for myoelectric control [21]. Then, root-mean-square (RMS) envelopes of the windows were used to train the models.

C. Experimental Procedures

Subjects were instructed to perform the motions displayed on a monitor with moderate force to prevent muscle fatigue. In experiments with *donees*, some timing differences were observed between the measured signals and displayed motion owing to the unfamiliarity of the subjects with sEMG signal measurement. Therefore, the sEMG signals were manually segmented.

Signals during resting conditions were measured to train the model for noise reduction. This technique helps minimize the effects of environmental conditions, such as skin impedance variations due to skin conditions.

Target motions for the muscle source activation model identification and u/d for compensation were performed. The subjects were asked to perform for $3\,\mathrm{s}$, and the last signal of $2\,\mathrm{s}$ was used.

Afterward, each target motion was repeated for $15\,\mathrm{s}$, where the contraction speed was not fixed. These signals were used to train the model on the relationship between source activation and motion intensity.

The model on the relationship between the motion intensity and gesture was trained using single-layer perceptron. Then, the offline classification performance was evaluated.

All procedures were conducted using MATLAB 2018a. Specific MATLAB functions used to construct models are described in our previous works [12]–[15].

D. Previous Works

This section briefly describes our previously proposed methods for baseline noise reduction and motion intensity extraction.

1) Baseline noise reduction: A baseline noise diminishes the quality and reliability of sEMG signals. We developed a noise reduction technique to eliminate a specific noise that has a periodic pattern. The noise reduction is conducted in the frequency domain as follows:

$$
\begin{aligned}
y &= \mathrm{fft}(x) \\
|y'| &= \begin{cases} |y| - Y_{\text{noise}}, & \text{if } (|y| - Y_{\text{noise}}) \geq 0 \\ 0, & \text{otherwise} \end{cases} \\
\angle y' &= \angle y \\
x' &= \mathrm{ifft}(y')
\end{aligned} \tag{1}
$$

where x denotes the measured sEMG signal in windows; y denotes the converted signal in the frequency domain; Y_{noise} denotes the noise parameters; and x' denotes the noise-reduced signal. Y_{noise} can be obtained as follows:

$$
\begin{aligned}
y^j_{\text{noise}} &= \mathrm{fft}(x^j_{\text{noise}}) \\
Y^l_{\text{noise}} &= \max_{1 \leq j \leq J} |y^{lj}_{\text{noise}}|, \quad l = 1, \cdots, L
\end{aligned} \tag{2}
$$

where J denotes the number of windows extracted from a noise signal; x_{noise} and y^j_{noise} denote an sEMG signal and its converted form in the jth window, respectively; $|y^{lj}_{\text{noise}}|$ denotes the amplitude of the lth frequency component computed in the jth window of the noise signal; and L denotes the window length.

The proposed technique can reduce not only baseline noise but also crosstalk noises, as described in [15]. However, this study focused only on baseline noise reduction.

2) Muscle source activation model: sEMG signals can be decomposed into source activations as follows:

$$
\begin{aligned}
V_{M_i} &= \sum_k ||d_{i_1 k} - d_{i_r k}| - |d_{i_2 k} - d_{i_r k}|| V_{S_k} \\
&= \sum_k D_{ik} V_{S_k}
\end{aligned} \tag{3}
$$

where V_{M_i} denotes the RMS envelope of a noise-reduced sEMG signal from the ith channel; and V_{S_k} denotes the kth source activation. $d_{i_1 k}$, $d_{i_2 k}$ and $d_{i_r k}$ denote the distance between the kth source and electrodes of ith channel (two active electrodes and one reference electrode), which is represented as follows:

$$
d_{ik} = 1 / \sqrt{\frac{(x_i - x_k)^2}{e^{\sigma_{x_k}}} + \frac{(y_i - y_k)^2}{e^{\sigma_{y_k}}} + \frac{(z_i - z_k)^2}{e^{\sigma_{z_k}}}} \tag{4}
$$

where x_i, y_i, z_i, and x_k, y_k, z_k denote the placement of the ith electrode and kth source, respectively; and σ_{x_k}, σ_{y_k}, and σ_{z_k} denote the directional conductivity of the kth source.

After parameter identification of D_{ik}, source activations can be extracted from sEMG signals.

3) Motion intensity extraction: Motion intensity was obtained by training the model on the relationship between source activations and a summation of RMS signals from all channels during repetitive muscle contractions for a particular motion as follows:

$$
\begin{aligned}
V^t_{MI} &= \sum_i V^t_{M_i} \quad i = 1, \cdots, N \\
&= net(\overline{V^t_S})
\end{aligned} \tag{5}
$$

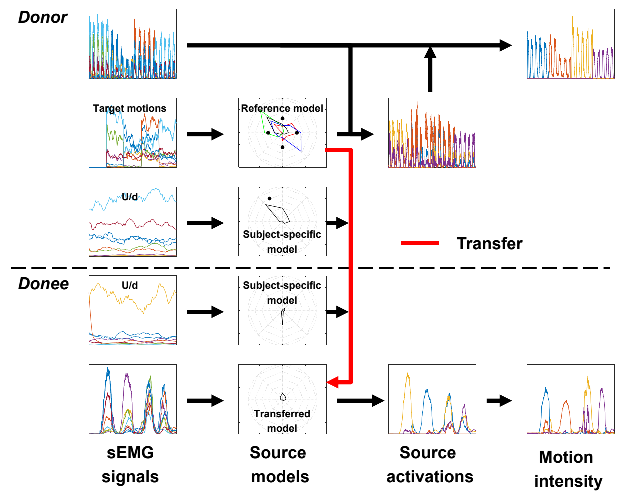

Fig. 2. A detailed scheme of the model-based parameter transfer.

where $V^t_{M_i}$ denotes the RMS envelope of a noise-reduced sEMG signal from the ith channel during repetitive dynamic muscle contractions for a particular t motion; N denotes the number of sEMG channels; V^t_{MI} denotes the motion intensity for a particular t motion; and $\overline{V^t_S}$ denotes a set of source activations, where each source activation was normalized by a maximum magnitude in a training set.

E. Reference Model-Based Parameter Transfer

The source parameters consist of the conductivity and location. These parameters are subject-dependent in the case of a conventional model, i.e., a subject-specific model. To obtain the subject-independent model parameters, a reference model was developed. The model has four equally distributed sources that have a constant conductivity of 0. The placements of reference sources were arbitrarily set; and the distance between a source and origin was $25\,\mathrm{mm}$.

Source activations corresponding to each motion can be extracted based on a reference model in the same manner as the conventional approach described in [12]–[15]. Afterward, the model on the relationship between motion intensity and gestures is trained.

Parameter transfer to other subjects requires a single-step procedure, i.e., rotation compensation that can be performed based on subject-specific muscle source activation model parameters considering only u/d.

In conclusion, parameter transfer requires two muscle source activation models from a *donor*: a reference model for target motions and a subject-specific model that only considers the u/d.

A detailed scheme of the muscle source activation model-based parameter transfer is shown in Fig. 2.

III. Results

This section can be divided into two main parts. Part one (Sections III-A to III-C) describes how parameter transfer works. The figures in this section were obtained from subjects 1 and 2 as a *donee* and *donor*, respectively. Part two (Sections III-D to III-E) addresses the performance of the

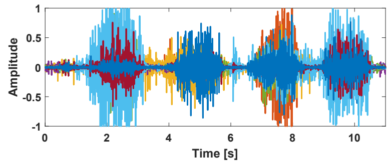

(a) Raw signals

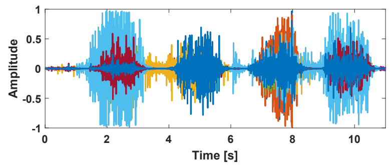

(b) Noise-reduced signals

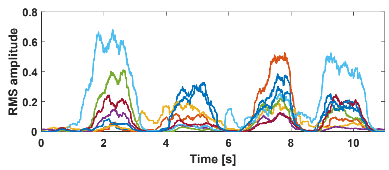

(c) RMS envelopes of (b)

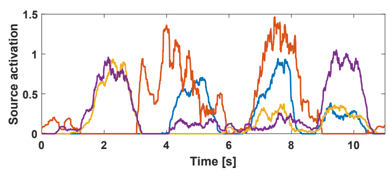

(d) Normalized source activations

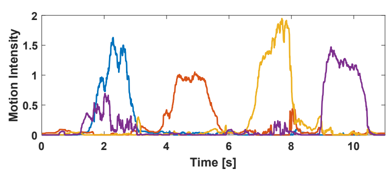

(e) Motion intensity

Fig. 3. Signals obtained from a *donor*. Target motions were performed sequentially. Motion intensity, extracted from sEMG signals, shows high selectivity according to the corresponding motion. Each colored line represents one of the signals from sEMG channels ((a) to (c)) or extracted signals ((d) and (e)).

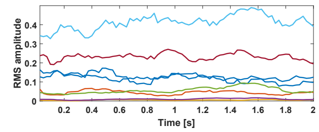

(a) sEMG signals from a *donor*

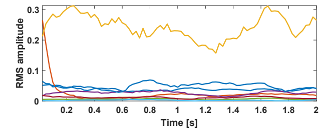

(b) sEMG signals from a *donee*

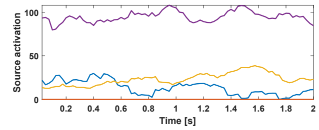

(c) Extracted source activations corresponding to (a)

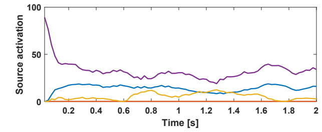

(d) Compensated source activations corresponding to (b)

Fig. 4. Measured sEMG signals and corresponding source activations obtained using a reference model. Ulnar deviation-based rotation compensation was conducted on the *donee*. Each colored line represents one of the signals from sEMG channels.

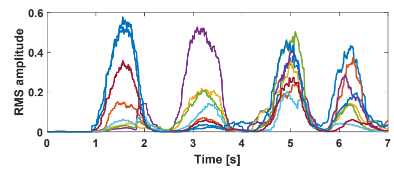

(a) RMS envelopes of noise-reduced sEMG signals

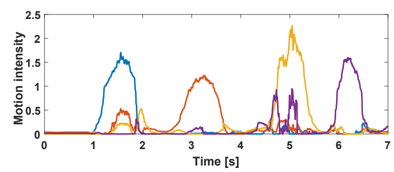

(b) Motion intensity

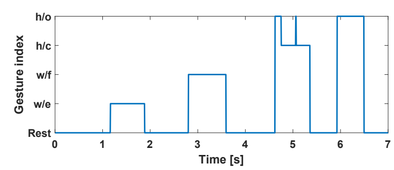

(c) Classified gesture

Fig. 5. sEMG signals, corresponding motion intensity, and classified gestures from a *donee*. Although sEMG signals showed a different pattern compared with those from a *donor*, the proposed method compensates for this difference. Each colored line represents one of the signals from sEMG channels (a) or extracted motion intensity (b).

subject-independent classification method; reference models were obtained from all *donors*, i.e., subjects in group A.

A. *sEMG Signals to Motion Intensity*

Fig. 3 describes sEMG signals and the corresponding noise-reduced signals, source activations, and motion intensity extracted from a *donor*; four target motions were conducted in sequence. Source activations (Fig. 3(d)) showed poor selectivity because the reference model failed to represent the anatomical factors of the subject. However, the highly selective features can be extracted by applying the motion intensity extraction method, as shown in Fig. 3(e).

B. *Parameter Transfer*

sEMG signals can be converted into source activations and motion intensity after the construction of a reference model. Fig. 4 describes the sEMG signals and converted source activations for u/d.

A *donor* and *donee* showed different sEMG patterns (Fig. 4(a) and (b)) because they have different muscle parameters, and there was a difference in interface rotation. However, despite these differences, similar source activations were obtained (Fig. 4(c) and (d)). The reference parameters were robust against anatomical differences, and the rotation compensation technique facilitated the transfer of parameters.

C. *Subject-Independent Gesture Recognition*

Fig. 5(a) describes sEMG signals obtained during sequentially performed target motions from a *donee*. The pattern is different from that of a *donor* (Fig. 3(c)) due to anatomical differences. The reference model compensated for the difference (Fig. 3(e) and Fig. 5(b)), and a reasonably classified gesture (Fig. 5(c)) was obtained.

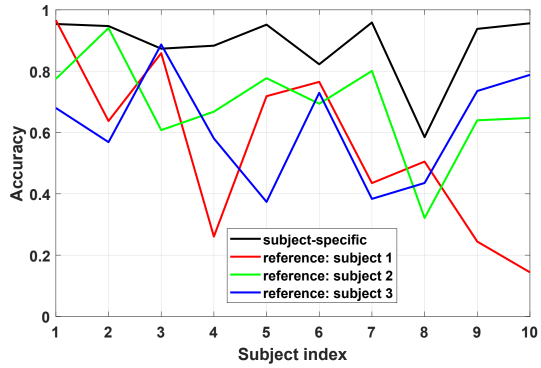

Fig. 6. Accuracy according to the reference model. The black line indicates the accuracy of the classifier, which was trained using each subject's RMS envelopes of sEMG signals (i.e., a subject-specific classifier without the application of the proposed method). Red, green, and blue lines indicate the accuracy obtained by using reference models from *donors*: subjects 1, 2, and 3.

In conclusion, the proposed reference model facilitates subject-independent gesture recognition.

D. Performance Evaluation

The proposed method was applied to all 10 subjects who participated in the experiment. Three reference models from *donors* (subjects in group A) were used. The classification accuracy according to each model is described in Fig. 6.

Classifiers trained using only each subject's own RMS envelopes of sEMG signals (i.e., a subject-specific classifier without the application of the proposed method) showed the highest accuracy in most cases; the average accuracy obtained from all subjects was $88.7\,\%$. The accuracy obtained using the proposed method depends on the reference model used and varied by user. For all cases, the average accuracy of the best and worst cases for each subject was $78.3\,\%$ and $42.8\,\%$, respectively.

The difference in accuracy could be attributed to the anatomical differences that the current model was unable to compensate for. As a part of the investigation, the relationship between the performance and angular differences of the interface is discussed in III-E.

E. Effect of Angular Difference

One possible reason for the performance degradation is that rotation compensation was not sufficient to fully transfer the model. Fig. 7 describes the relationship between the accuracy and angular differences of the interface between *donors* and *donees*. The interface rotation was measured using an IMU integrated with an MYO armband. The accuracy was normalized to subject-specific classification accuracy (Fig. 6, black line). As the angular difference increased, the accuracy decreased. Therefore, accuracy might increase with an advanced reference model.

IV. Discussion

A. Parameters for Reference Sources

In the proposed reference source model, both the number of sources and the source locations were arbitrarily fixed.

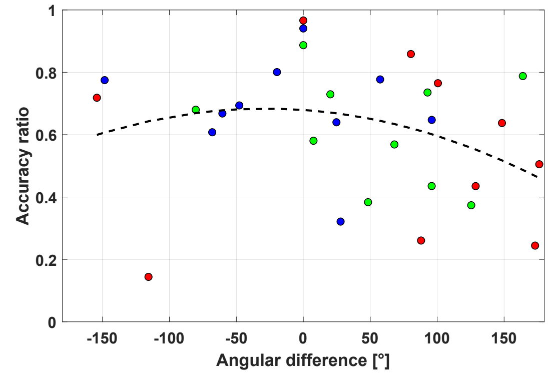

Fig. 7. Relationship between normalized accuracy and angular difference of the interface between *donors* and *donees*. Red, green, and blue points represent the adopted reference model from subjects 1, 2, and 3, respectively. The black dashed line indicates the fitted line with a second-degree polynomial.

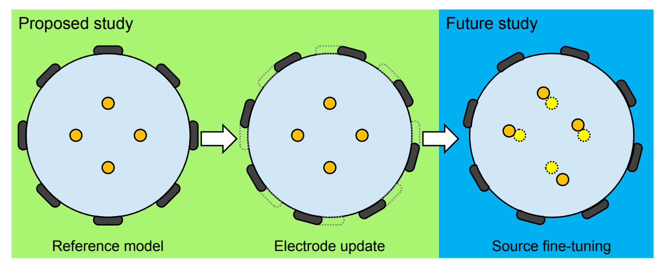

Fig. 8. Parameter tuning for subject-independent gesture recognition. Fine-tuning of source parameters is needed.

These predetermined parameters affect not only signal decomposition but also pattern recognition performance. The selection method for source parameters should be further investigated.

B. Limitation of Current Parameter Transfer

Parameter transfer is based on rotation compensation that only requires u/d motion; hence, simple and fast compensation is possible.

However, the anatomical difference cannot be compensated using only rotation compensation owing to significant variations. For this reason, the accuracy ratio fell below $20\,\%$ in the worst case, which is unacceptable. Therefore, an additional parameter transfer method is required to compensate for anatomical differences.

Fig. 8 shows the expected parameter transfer method: the fine-tuning of source parameters, including source location and source conductivity. In the case of rotation compensation, all relationships between sources and electrodes were changed simultaneously. In the case of fine-tuning, each source parameters will be adjusted independently.

C. Additional Experiments Needed

Reference models were constructed from three subjects; each subject had a different level of familiarity with sEMG signal measurements. We expected the subject who was highly familiar with sEMG signal measurements to develop a more reliable reference model than the subject with less familiarity. However, the correlation between familiarity and performance was weak.

Anatomical factors, such as muscle size and length, might affect the performance. However, in this study, only the effect of the angular difference of the interface between a *donor* and *donee* was considered; thus, additional parameters should be investigated.

Experiments with more subjects considering additional wrist/hand motions frequently used in daily activities [22] should be conducted to further validate the proposed approach. In addition, real-time estimations should be performed.

D. Working on Amputees

One limitation of this study is that the proposed method was applied only on non-amputees. There are anatomical differences between non-amputee and amputee subjects; for example, the muscle activity of residual limbs of amputees may differ from that of intact limbs. Therefore, it remains uncertain whether the proposed method is applicable to the amputee population.

V. Conclusions

This study proposed a subject-independent pattern recognition method based on a muscle source activation model. The conventional model has subject-specific source parameters that cannot be applied to other subjects. To overcome this limitation, we developed a reference model for subject-independent processing.

A proposed method facilitates not only subject-independent classification but also interface rotation-independent processing. A new user can utilize sEMG signals for motion recognition by simply wearing an interface and performing a single motion.

To demonstrate the performance, subject-independent classification was conducted for 10 subjects. The results demonstrated the feasibility of the proposed method. However, additional experiments and concrete theoretical backgrounds are required to further validate our proposed approach.

We expect that our proposed method will be able to enhance the practicability of sEMG-assisted applications. For instance, an amputee can adapt easily to a prosthetic hand with less effort, and intuitive teleoperation can be achieved with less configuration time, as compared to the exiting methods.

References

[1] L. Resnik, H. H. Huang, A. Winslow, D. L. Crouch, F. Zhang, and N. Wolk, "Evaluation of emg pattern recognition for upper limb prosthesis control: a case study in comparison with direct myoelectric control," *Journal of neuroengineering and rehabilitation*, vol. 15, no. 1, p. 23, 2018.

[2] Z. O. Khokhar, Z. G. Xiao, and C. Menon, "Surface emg pattern recognition for real-time control of a wrist exoskeleton," *Biomedical engineering online*, vol. 9, no. 1, p. 41, 2010.

[3] T. A. Schuler, R. Müller, and H. J. Van Hedel, "Leg surface electromyography patterns in children with neuro-orthopedic disorders walking on a treadmill unassisted and assisted by a robot with and without encouragement," *Journal of neuroengineering and rehabilitation*, vol. 10, no. 1, p. 78, 2013.

[4] A. J. Young, L. J. Hargrove, and T. A. Kuiken, "The effects of electrode size and orientation on the sensitivity of myoelectric pattern recognition systems to electrode shift," *IEEE Transactions on Biomedical Engineering*, vol. 58, no. 9, pp. 2537–2544, 2011.

[5] A. Boschmann, P. Kaufmann, M. Platzner, and M. Winkler, "Towards multi-movement hand prostheses: Combining adaptive classification with high precision sockets," in *Proceedings of the 2nd European Conference Technically Assisted Rehabilitation*. Citeseer, 2009.

[6] K. Watanabe, M. Kouzaki, M. Ogawa, H. Akima, and T. Moritani, "Relationships between muscle strength and multi-channel surface emg parameters in eighty-eight elderly," *European Review of Aging and Physical Activity*, vol. 15, no. 1, p. 3, 2018.

[7] T. W. Beck, T. J. Housh, J. T. Cramer, and J. P. Weir, "The effect of the estimated innervation zone on emg amplitude and center frequency," *Medicine & Science in Sports & Exercise*, vol. 39, no. 8, pp. 1282–1290, 2007.

[8] A. Gallina, R. Merletti, and M. Gazzoni, "Innervation zone of the vastus medialis muscle: position and effect on surface emg variables," *Physiological measurement*, vol. 34, no. 11, pp. 1411–1422, 2013.

[9] T. Tommasi, F. Orabona, C. Castellini, and B. Caputo, "Improving control of dexterous hand prostheses using adaptive learning," *IEEE Transactions on Robotics*, vol. 29, no. 1, pp. 207–219, 2012.

[10] N. Patricia, T. Tommasit, and B. Caputo, "Multi-source adaptive learning for fast control of prosthetics hand," in *2014 22nd International Conference on Pattern Recognition*. IEEE, 2014, pp. 2769–2774.

[11] U. Côté-Allard, C. L. Fall, A. Drouin, A. Campeau-Lecours, C. Gosselin, K. Glette, F. Laviolette, and B. Gosselin, "Deep learning for electromyographic hand gesture signal classification using transfer learning," *IEEE Transactions on Neural Systems and Rehabilitation Engineering*, vol. 27, no. 4, pp. 760–771, 2019.

[12] M. Kim and W. K. Chung, "Muscle activation source model-based semg signal decomposition and recognition of interface rotation," in *2018 IEEE/RSJ International Conference on Intelligent Robots and Systems (IROS)*. IEEE, 2018, pp. 2780–2786.

[13] M. Kim, K. Kim, and W. K. Chung, "Simple and fast compensation of semg interface rotation for robust hand motion recognition," *IEEE Transactions on Neural Systems and Rehabilitation Engineering*, vol. 26, no. 12, pp. 2397–2406, 2018.

[14] M. Kim, W. K. Chung, and K. Kim, "Preliminary study of virtual semg signal-assisted classification," in *2019 IEEE 16th International Conference on Rehabilitation Robotics (ICORR)*. IEEE, 2019, pp. 1133–1138.

[15] ——, "Motion intensity extraction scheme for simultaneous recognition of wrist/hand motions," in *2020 IEEE International Conference on Robotics and Automation (ICRA)*. IEEE, 2020, pp. 10 112–10 117.

[16] J. DelPreto, A. F. Salazar-Gomez, S. Gil, R. M. Hasani, F. H. Guenther, and D. Rus, "Plug-and-play supervisory control using muscle and brain signals for real-time gesture and error detection." in *Robotics: Science and Systems*, 2018.

[17] J. DelPreto and D. Rus, "Plug-and-play gesture control using muscle and motion sensors," in *Proceedings of the 2020 ACM/IEEE International Conference on Human-Robot Interaction*, 2020, pp. 439–448.

[18] L. Pan, D. Zhang, N. Jiang, X. Sheng, and X. Zhu, "Improving robustness against electrode shift of high density emg for myoelectric control through common spatial patterns," *Journal of neuroengineering and rehabilitation*, vol. 12, no. 1, p. 110, 2015.

[19] Coapt gen 2 complete control system. [Online]. Available: https://coaptgen2.com/

[20] A. M. Simon, B. A. Lock, and K. A. Stubblefield, "Patient training for functional use of pattern recognition–controlled prostheses," *Journal of prosthetics and orthotics: JPO*, vol. 24, no. 2, pp. 56–64, 2012.

[21] L. H. Smith, L. J. Hargrove, B. A. Lock, and T. A. Kuiken, "Determining the optimal window length for pattern recognition-based myoelectric control: balancing the competing effects of classification error and controller delay," *IEEE Transactions on Neural Systems and Rehabilitation Engineering*, vol. 19, no. 2, pp. 186–192, 2010.

[22] I. M. Bullock, J. Z. Zheng, S. De La Rosa, C. Guertler, and A. M. Dollar, "Grasp frequency and usage in daily household and machine shop tasks," *IEEE transactions on haptics*, vol. 6, no. 3, pp. 296–308, 2013.